



Research article

Deficiency of protein phosphatase 5 resists osteoporosis in diabetic mice

Jun Wang^a, Changyu Zhao^a, Wenpeng Zhao^a, Songnan Li^{b,*}

^a School of Tourism and Cuisine, Yangzhou University, Yangzhou 225127, China

^b Joint International Research Laboratory of Agriculture and Agri-Product Safety of the Ministry of Education of China, Institutes of Agricultural Science and Technology Development, Yangzhou University, Yangzhou 225009, China

ARTICLE INFO

Keywords:

Osteoporosis
Diabetes
High-fat diet
Protein phosphatase 5
Osteoblast
Osteoclast

ABSTRACT

Osteoporosis is a common diabetic consequence that negatively affects patients' health and quality of life. Nevertheless, there is mutual interference between clinical drugs intended to regulate blood glucose and bone metabolism. Therefore, it is crucial to look for new treatment targets that effectively control blood glucose and safely protect the bone health of patients with diabetes. In this study, mice given a high-fat diet were shown to be resistant to osteoporosis and diabetes when protein phosphatase 5 (PP5) knockout (KO) mice were used. Serum markers of bone remodeling show that PP5 KO mice are resistant to decreased bone formation and increased bone resorption brought on by diabetes. The absence of PP5 resists the reduction of osteoblast differentiation and the enhancement of osteoclast differentiation in diabetic mice, according to the *in vitro* osteoblast differentiation of bone mesenchymal stem cells and osteoclast differentiation of bone marrow-derived macrophages. Subsequent investigation revealed that PP5 deficiency increases the expression of the key regulator of osteoblast differentiation, runt-related transcription factor 2, and decreases the activity of the receptor activator of the nuclear factor- κ B ligand/osteoprotegerin pathway, a crucial regulatory signaling pathway for osteoclast differentiation. In conclusion, we discovered that PP5 deficiency protects diabetic mice against osteoporosis for the first time.

1. Introduction

The prevalence of diabetes, a chronic metabolic disorder that seriously endangers public health, is rising yearly. Osteoporosis is a diabetic consequence affecting a patient's health and quality of life [1,2]. A systemic metabolic bone disease, osteoporosis is defined by poor bone remodeling, which raises the risk of bone fractures by reducing bone mass, altering the microstructure of bone tissue, weakening bones, and increasing susceptibility to fractures [3–5]. In mature animals, the process of bone remodeling, in which bone tissue goes through an ongoing cycle of absorption and reconstruction determines the quality of the skeletal system [6–8]. A dynamic balance between bone creation and resorption exists in healthy bone tissue, which is essential for preserving the quality of the bone [9]. But when diabetes worsens, this equilibrium is upset, leading to a shift in bone remodeling toward more resorption, a decrease in bone turnover rates, and progressive deterioration of bone quality in those impacted [10–13]. Nowadays, therapeutic blood glucose controlling drugs include sodium-glucose cotransporter 2 inhibitors, thiazolidinediones, and sulfonylureas; however, long-term use of

* Corresponding author.

E-mail address: lsnyz2020@yzu.edu.cn (S. Li).

<https://doi.org/10.1016/j.heliyon.2024.e34027>

Received 3 February 2024; Received in revised form 23 June 2024; Accepted 2 July 2024

Available online 2 July 2024

2405-8440/© 2024 The Authors. Published by Elsevier Ltd. This is an open access article under the CC BY-NC-ND license (<http://creativecommons.org/licenses/by-nc-nd/4.0/>).

these drugs may put diabetic patients' bone health at risk [14–17]. Therefore, the quest for new therapeutic targets capable of controlling blood glucose levels and protecting the bone health of individuals with diabetes is fundamental. Previous research has demonstrated that animals deficient in protein phosphatase 5 (PP5) are resistant to the effects of a high-fat diet on weight gain and diabetes [18–21]. Studies have shown that PP5 dephosphorylates the peroxisome proliferator-activated receptor γ (PPAR γ) and the glucocorticoid receptor, which controls the metabolism of glucose and fat [19–21]. According to our earlier research, PP5 has a negative regulatory effect on mouse osteogenesis [22]. According to a biochemical study, PP5 modulates the dephosphorylation of runt-related transcription factor 2 (RUNX2) and PPAR γ , negatively affecting osteogenic differentiation [22]. Nonetheless, little information about how PP5 affects osteoclast development and bone resorption is available. As PP5 regulates glucose and bone growth, it is a promising dual target for treating skeletal diseases and diabetes. This study used PP5 knockout (KO) mice as experimental subjects and created a diabetic mouse model using a prolonged high-fat diet and streptozotocin injections to investigate the effects of PP5 on the bone tissue of diabetic mice. The findings of this study will offer a strong theoretical framework for investigating possible treatment targets for diabetes and the associated problems connected to bone health.

2. Materials and methods

2.1. Experimental animals

On a C57BL/6 genetic background, PP5 KO mice and wild-type (WT) littermates were bred [23]. The Ethics Committee of Yangzhou University approved all animal experiments. Additionally, the animal ethics permit number is NSFC2020-LPSPXY-3.

2.2. Diabetes mouse models

A total of 30 PP5 KO male mice and 30 WT male mice, aged 10 weeks, were randomly assigned to four groups: WT normal control (WT-NC), WT diabetic mellitus (WT-DM), KO normal control (KO-NC), and KO diabetic mellitus (KO-DM). A high-fat diet of 60 % fat was given to the mice in the DM groups, whereas the NC groups were given a standard diet. After 2-weeks of dietary regimen, the mice in the high-fat diet groups were subjected to intraperitoneal injections of streptozotocin in a sodium citrate buffer (40 mg/kg/day) for 5 days. For 20 weeks, the mice were kept under observation, and their body weight was measured weekly. Following a high-fat diet, fasting blood glucose levels were measured in all groups using the Roche blood glucose meter (F. Hoffmann-La Roche, Ltd., Basel, Switzerland).

2.3. Glycated hemoglobin and insulin

Serum was extracted from the retro-orbital venous plexus using blood samples from three mice selected from each group. ELISA test kits (Jiancheng Biotechnology Co., Ltd., Nanjing, China) were used to determine the amounts of insulin and hemoglobin A1c (HbA1c) in serum.

2.4. Oral glucose tolerance test (OGTT) and insulin tolerance test (ITT)

At the twentieth week, six mice from each group were given 0.5 g/kg of body weight of glucose orally via gavage for OGTT following a 16-h fast. For ITT, these mice were given insulin (Solarbio, Beijing, China) at a dose of 1 U/kg of body weight after fasting for 6 h 2 days following OGTT. After administering glucose at 0, 15, 30, 60, and 120 min, the blood glucose levels in these two tests were recorded, and the blood glucose area under the curve (AUC) was computed.

2.5. Bone remodeling markers

Serum was extracted by drawing blood from the retro-orbital venous plexus. Receptor activator of nuclear factor- κ B ligand (RANKL), carboxy-terminal telopeptide of type-I collagen (CTX-1C), propeptide of type I procollagen (PINP), osteocalcin (OCN), and osteoprotegerin (OPG) were among the markers of bone remodeling whose serum concentrations were measured using ELISA assay kits (Yuanxin Biotechnology Co., Ltd., Shanghai, China).

2.6. Micro-CT scanning

Bilateral femurs of mice were immediately scanned to evaluate changes in bone microstructure using PIXImus CT (Siemens, WA, USA).

2.7. Osteoblast differentiation

Following the previously described procedure [22], bone mesenchymal stem cells (BMSCs) from bone fragments of mouse femurs were harvested and seeded at a density of 5×10^3 /mL into 24-well plates. The 24-well plates were filled with osteoblast differentiation solution (MEM- α culture medium containing 10 mmol/mL of β -glycerol phosphate and 25 μ mol/mL of ascorbic acid) to produce osteoblasts [22]. Alizarin red staining was carried out following a 21-day differentiation period.

2.8. Osteoclast differentiation

Following reference [24], bone marrow-derived macrophages (BMMs) were produced using accepted literature references and then stimulated to develop into osteoclasts. The BMMs (1.5×10^5 /mL) were cultured in MEM- α complete culture medium containing macrophage colony stimulating factor (MCSF) (5 ng/mL; R&D Systems company, Minneapolis, MN, USA) for 3 days, followed by further incubation in fully differentiated medium containing MCSF (30 ng/mL) and RANKL (60 ng/mL; R&D Systems company, Minneapolis, MN, USA). On the ninth day, the differentiation of the osteoclasts was assessed by TRAP staining (Yangming Biotechnology Co., Ltd, Hangzhou, China).

2.9. Capability of osteoclast bone resorption

For differentiation culture, BMMs (2×10^5 /mL) were seeded into 24-well plates containing cow bone slices. The bone slices were carefully removed on the ninth day of differentiation, cleaned, fixed for 2 h with 2.5 % glutaraldehyde, and then dried with ethanol. Next, bone resorption pits were seen and photographed using a Hitachi, Tokyo, Japan, S-4800II field emission scanning electron microscope.

2.10. BMSCs-BMMs co-cultured to induce osteoclast differentiation

A density of 5×10^3 /mL of BMSCs was added to 24-well plates for inoculation. The 24-well plates were filled with osteoblast differentiation solution and left for 7 days to harvest osteoblasts. Following established protocols [25], bone marrow was used to extract BMMs, which were injected at a density of 5×10^4 /mL into the osteoblast culture dish. The solution was substituted with the MEM- α culture media containing 1,25-(OH) $_2$ D $_3$ (10^{-8} M) (Sigma-Aldrich, St. Louis, MO, USA) and macrophage colony-stimulating factor (25 ng/mL) (R&D Systems, Minneapolis, MN, USA) to stimulate osteoclast differentiation. TRAP (Yangming, Hangzhou, China) staining was used on the ninth day of osteoclast differentiation to examine the impact of osteoblasts on osteoclast differentiation.

2.11. Concentrations of OPG and RANKL in osteoblasts

An osteoblast differentiation solution was used for 14 days to differentiate WT and KO BMSCs into osteoblasts. Forty μ M arachidonic acid (AA) (Sigma-Aldrich, St. Louis, MO, USA) was given to a fraction of WT osteoblasts for 2 h to activate PP5. Also, ELISA assay kits (Yuanxin Biotechnology Co., Ltd., Shanghai, China) were used to measure the amounts of OPG and RANKL in the WT, KO, and WT + AA osteoblasts culture medium.

2.12. Quantitative real-time polymerase chain reaction

Mouse femurs were used to extract total mRNA using Trizol, and TaKaRa Biotechnology Co. Ltd., Dalian, China, provided the kit for cDNA synthesis. Quantitative real-time PCR was used using the primers listed in Table 1.

2.13. Western blot

Using conventional techniques, the BCA assay kit (Beyotime, Shanghai, China) was used to measure the protein concentration after the total protein was isolated from mice femur [26]. Standard techniques were used to carry out the Western blot analysis. Utilizing

Table 1
Quantitative Real-Time PCR primers.

Primer	Sequence
<i>Nfatc1</i>	F: 5'-CACTCCACCCACTTCTGACTTCC-3' R: 5'-GGCTGCCTTCGGTCTCATAGTG-3'
<i>Opg</i>	F: 5'-CCCTTGCCCTGACCACTTAT-3' R: 5'-AGGGTGCTTTCGATGAAGTCTCA-3'
<i>Rankl</i>	F: 5'-CCATCGGGTCCCATAAAGTCA-3' R: 5'-CAGTTTTTCGTGCTCCCTCCTT-3'
<i>Ocn</i>	F: 5'-GACCTCACAGATGCCAAGCCC-3' R: 5'-ATAGATGCGTTTGTAGGCGGC-3'
<i>Bsp</i>	F: 5'-CCAGCCAGAAAGAGCAGC-3' R: 5'-CCTCGTAGCCTTCATAGCC-3'
<i>Runx2</i>	F: 5'-CATTGCACTGGGTCCACACGTA-3' R: 5'-GAATCTGGCCATGTTTGTGCTC-3'
<i>Pp5</i>	F: 5'-AACAAGATCGTGAAGCAGAAGGCC-3' R: 5'-TTCGTGGCTGCGGATGATATAGTC-3'
<i>Gapdh</i>	F: 5'-CCTCGTCCCGTAGACAAAATG-3' R: 5'-TGAGGTCAATGAAGGGTCGT-3'

RUNX2-antibody (Santa Cruz, CA, USA) changes in protein expression were evaluated.

2.14. Statistical methods

GraphPad Prism 8.0.2 was used to do data differential analysis. Two-way Analysis of variance (ANOVA) was utilized for comparisons involving several groups, while the Student's t-test was used for comparisons between two groups.

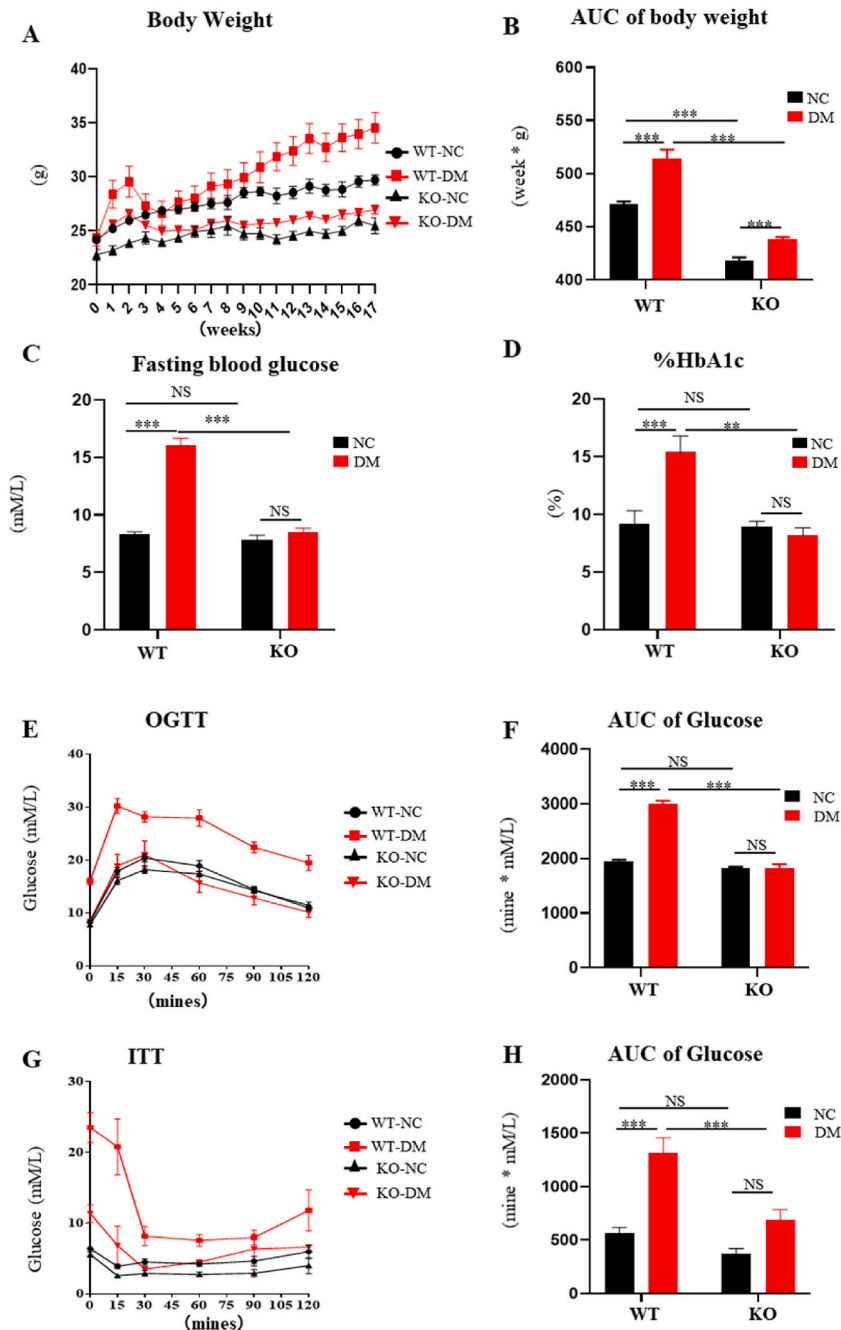


Fig. 1. PP5 deficiency resists high-fat diet-induced diabetes. Body weights of mice in each group (A), and the area under the curve (AUC) (B). Fasting blood glucose (C), HbA1c (D), oral glucose tolerance (E), insulin tolerance (G), and the AUC of blood glucose in OGTT (F) and ITT (H). Each value represents mean ± SD (n = 6). *: P < 0.05; **: P < 0.01; ***: P < 0.001; NS: P > 0.05.

3. Results

3.1. PP5 deficiency resists high-fat diet-induced diabetes

As the feeding time went on, the difference between the two groups' growth curves grew, with the mice from the WT-NC group continuously showing a higher growth curve than the KO-NC mice (Fig. 1A). Beginning in the eleventh week, the body weight of WT-DM mice grew more quickly than that of WT-NC mice (Fig. 1A). But as shown in Fig. 1A, the growth curve of KO-DM mice constantly matched that of KO-NC mice. Fig. 1B, $P < 0.001$, indicates that KO-NC mice had a considerably lower body weight than WT-NC mice based on the AUC for body weight in each group. Both WT and KO mice displayed a considerable increase in body weight after high-fat feeding (Fig. 1B, $P < 0.001$ and Fig. 1B, $P < 0.001$). However, when KO-DM mice were compared to WT-DM mice, their body weight was noticeably reduced (Fig. 1B, $P < 0.001$). All WT-DM mice's fasting blood glucose levels (>11.1 mmol/L) at the end of the high-fat diet satisfy the criteria for diabetes. KO-DM mice, on the other hand, continued to have fasting blood glucose levels below 11.1 mmol/L (Fig. 1C). Each mouse group's trend in HbA1c levels matched its fasting blood glucose levels (Fig. 1D). WT-NC and KO-NC mice had comparable blood glucose curves in the OGTT experiment. However, the blood glucose curve of WT-DM mice was noticeably higher than that of WT-NC mice following the high-fat diet. On the other hand, the blood glucose curves of WT-NC and KO-DM mice resembled each other quite a bit (Fig. 1E). Fig. 1F displays the statistical analysis of the blood glucose AUC for each group. Compared to WT-NC mice, the blood glucose AUC of WT-DM mice was considerably greater ($P < 0.001$). In the meantime, the blood glucose AUC of KO-DM mice was significantly lower than that of WT-DM mice and did not show any significant change when compared to KO-NC (Fig. 1F, $P < 0.001$). The ITT experiment noted comparable outcomes (Fig. 1G and H).

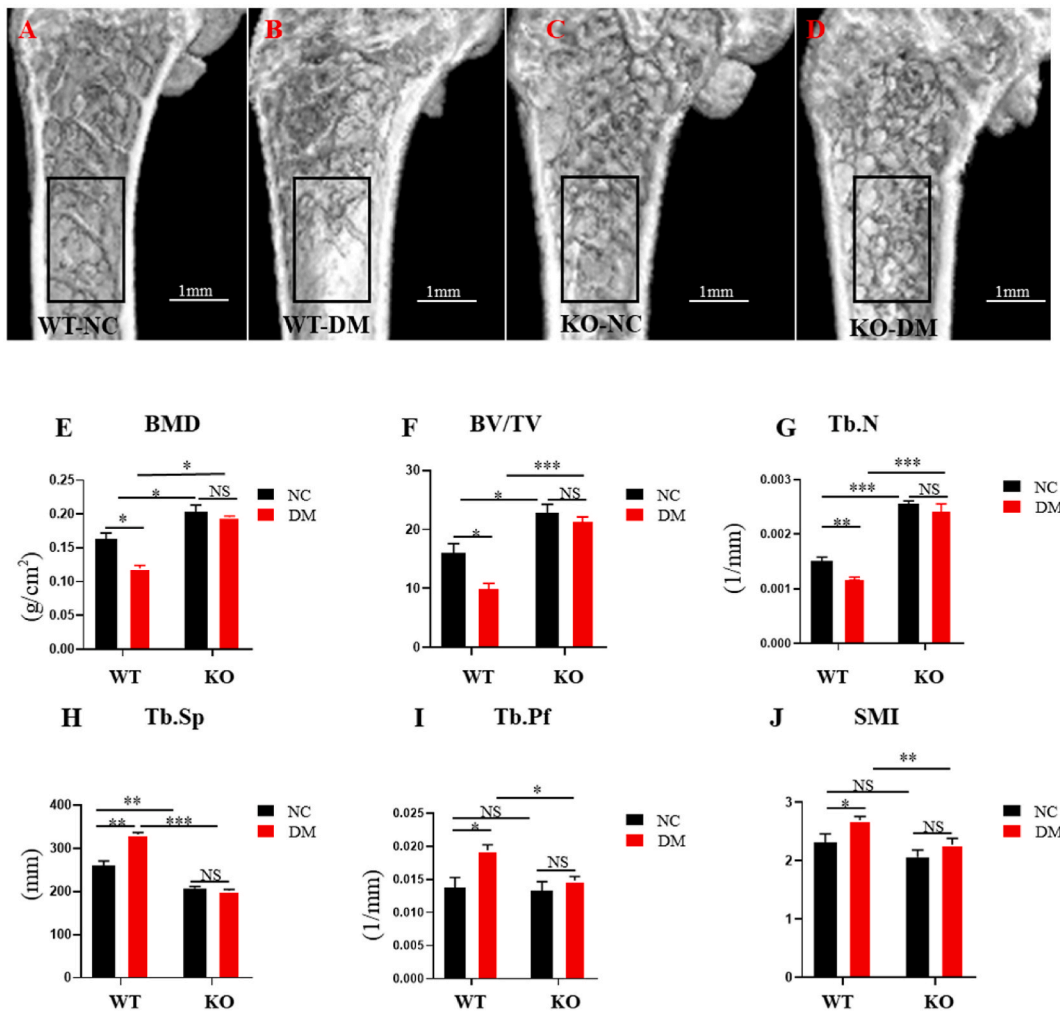


Fig. 2. PP5 deficiency resists osteoporosis in diabetic mice. At the end of the experiment, changes in bone microstructure were detected by micro-CT (A–D). Changes in bone microstructural parameters were statistically analyzed: bone mineral density (BMD) (E), bone volume fraction (BV/TV) (F), trabecular number (Tb.N) (G), trabecular separation (Tb.Sp) (H), trabecular pattern factor (Tb.Pf) (I) and structural pattern index (SMI) (J). Each value represents mean \pm SD (n = 3). *: $P < 0.05$; *: $P < 0.01$; *: $P < 0.001$; NS: $P > 0.05$.

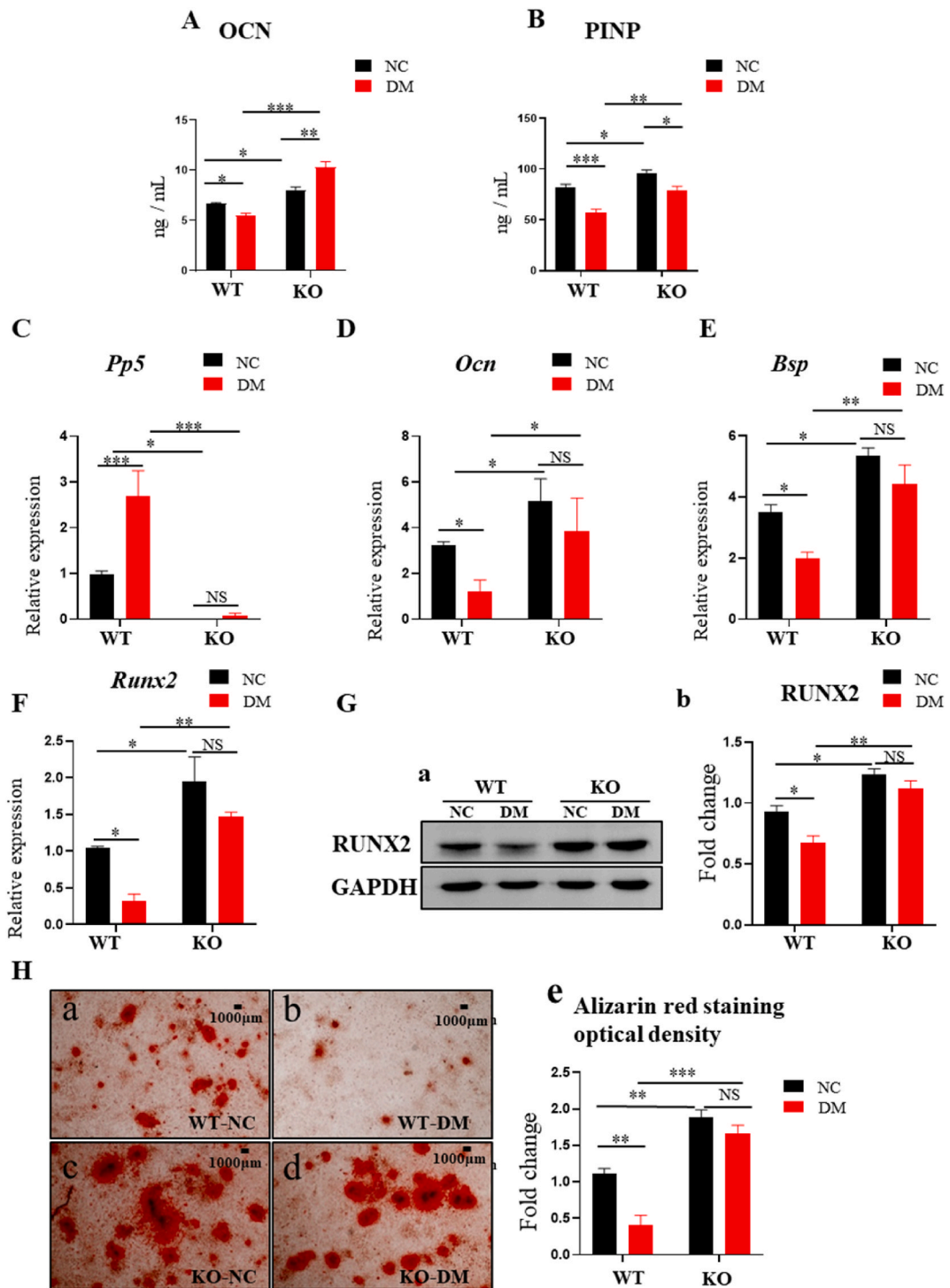


Fig. 3. Changes in bone formation and osteoblast differentiation in diabetic mice after PP5 deficiency. The serum concentrations of OCN (A) and PINP (B). The mRNA expression of *Pp5*(C), *Ocn* (D) and *Bsp* (E) *Runx2* (F) in the femurs of mice in each group. The expression of RUNX2 (G-a, b). BMSCs of mice in each group were induced to differentiate into osteoblasts in vitro and stained with alizarin red (H-a, b, c, d), and the area of calcium nodules was statistically analyzed (G-e). Each value represents mean \pm SD (n = 3). *: $P < 0.05$; **: $P < 0.01$; ***: $P < 0.001$; NS: $P > 0.05$. (For interpretation of the references to colour in this figure legend, the reader is referred to the Web version of this article.)

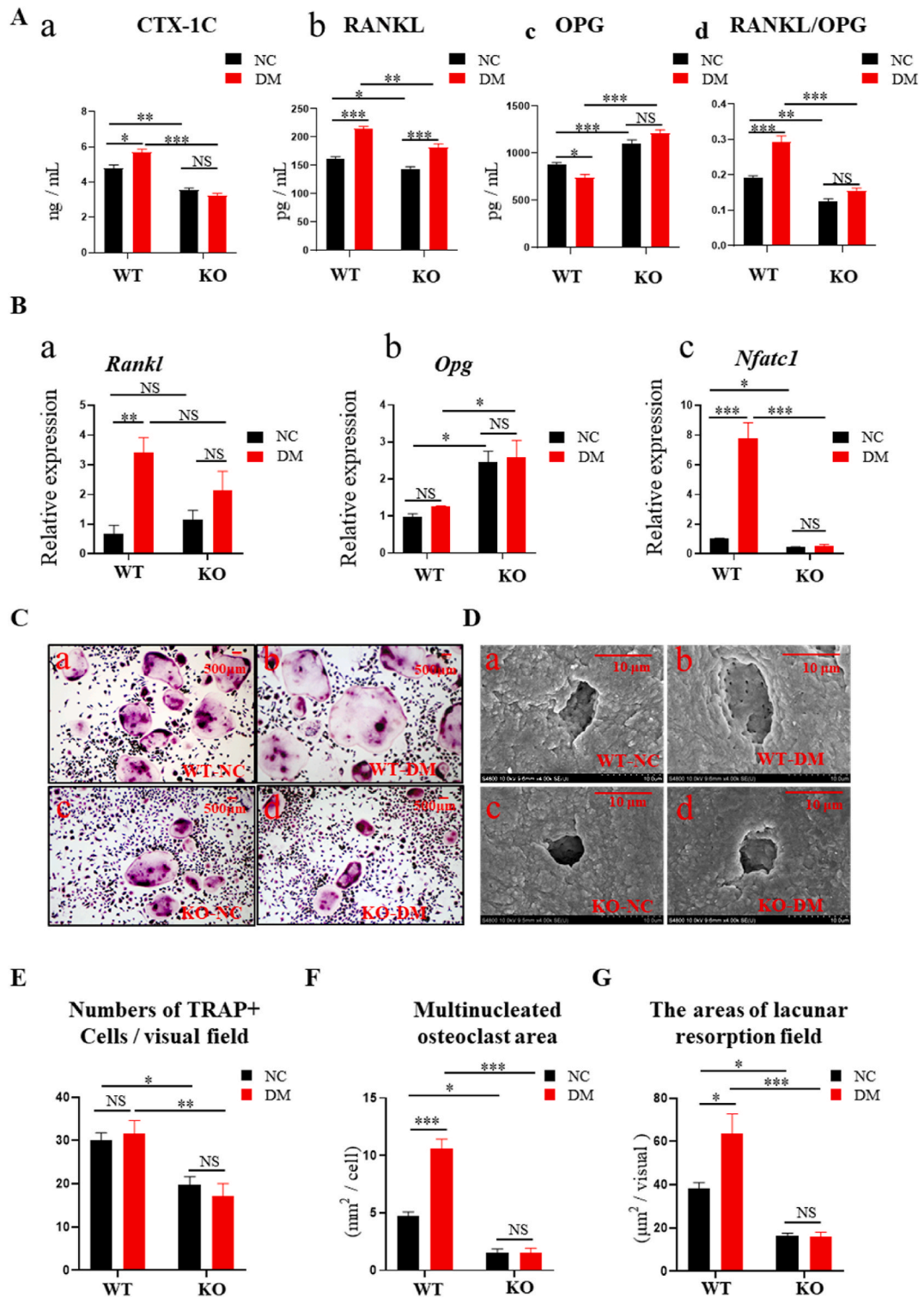


Fig. 4. Changes in osteoclast differentiation and bone resorption in diabetic mice. Serum levels of the bone resorption markers: CTX-1C (A-a), RANKL (A-b), OPG (A-c), and the ratio of RANKL/OPG (A-d) in each group of mice. Expression of *Opg*, *Rankl* and *Nfatc1* (B-a, b, c). BMMs were induced to differentiate into osteoclasts in vitro and subjected to TRAP staining (C-a, b, c, d) and statistically analyzed for the number (E) and area (F) of osteoclasts (within an area of 80 mm²). The resorption pits of osteoclasts differentiated from BMMs in mice of each group (D, G). Each value represents mean ± SD (n = 3). *: P < 0.05; **: P < 0.01; ***: P < 0.001; NS: P > 0.05.

3.2. PP5 deficiency resists osteoporosis in diabetic mice

Trabecular bone density in KO-NC mice was found to be considerably higher than in WT-NC mice, as demonstrated by micro-CT scans of the distal femur (Fig. 2A). Trabecular bone density at the distal femur was significantly lower in WT-DM mice than in WT-NC mice (Fig. 2A and B). Trabecular bone density did not significantly change in KO-DM mice relative to KO-NC mice (Fig. 2C and D). The results of the statistical analysis of the bone microstructural parameters in the different groups showed that the KO-NC mice were significantly different from the WT-NC mice in terms of bone mineral density (BMD), bone volume fraction (BV/TV), and trabecular number (Tb.N) (Fig. 2G, $P < 0.001$), as well as trabecular separation (Tb.Sp) (Fig. 2H, $P < 0.01$). Following the high-fat diet, the BMD (Fig. 2E, $P < 0.05$), BV/TV (Fig. 2F, $P < 0.05$), and Tb.N (Fig. 2G, $P < 0.01$) of WT-DM mice were considerably reduced; on the other hand, Tb.Sp (Fig. 2H, $P < 0.01$), trabecular bone pattern factor (Tb.Pf) (Fig. 2I, $P < 0.05$), and structure model index (SMI) (Fig. 2J, $P < 0.05$) were raised. In contrast, KO-DM mice exhibited no discernible alterations in the above mentioned measures (Fig. 2E, F, G, H, I, J).

3.3. PP5 deficiency protects bone formation in diabetic mice

The serum levels of OCN and PINP predict bone development and are significant markers of bone formation [27,28]. The serum concentrations of PINP (Fig. 3B, $P < 0.05$) and OCN (Fig. 3A, $P < 0.05$) in KO-NC mice indicated that bone formation was stronger in KO mice than in WT mice. Compared to WT-NC mice, these makers were significantly lower in WT-DM mice (OCN, Fig. 3A, $P < 0.05$; PINP, Fig. 3B, $P < 0.001$). But KO-DM mice had considerably greater serum levels of OCN than KO-NC (Fig. 3A, $P < 0.01$) and WT-DM (Fig. 3A, $P < 0.001$) mice. While PINP levels in the serum of KO-DM mice dramatically dropped (Fig. 3B, $P < 0.05$), they were still significantly greater than those of WT-DM mice (Fig. 3B, $P < 0.01$). These findings suggest that weaker bone development is caused by diabetic mellitus in WT mice, but that this impact is effectively blocked by PP5 lack. In bone tissues, *Pp5* expression shows that PP5 suppresses the bone formation in diabetic mice (Fig. 3C, $P < 0.05$). The femurs of KO-NC mice exhibited significantly higher expression of osteoblast markers in normal tissues, such as *Ocn* (Fig. 3D, $P < 0.05$), bone sialoprotein (*Bsp*) (Fig. 3E, $P < 0.05$), and runt-related transcription factor 2 (*Runx2*) [29] (Fig. 3F, $P < 0.05$), when compared to WT-NC mice. These findings suggest that PP5 KO mice may have significantly enhanced osteoblast differentiation. They were considerably lower in WT-DM mice following a high-fat diet than in WT-NC mice (Fig. 3D, E, F, $P < 0.05$). Nevertheless, the expression of these markers in KO-DM mice was considerably higher than in WT-DM mice (*Ocn*, Fig. 3D, $P < 0.05$; *Bsp*, Fig. 3E, $P < 0.01$; *Runx2*, Fig. 3F, $P < 0.01$) but not statistically different from KO-NC animals (Fig. 3D, E, and F). The alterations in RUNX2 protein found in the femurs of several mouse groups (Fig. 3G) align with the previously described qPCR outcomes. According to these findings, osteogenesis is suppressed in WT mice, by diabetes mellitus; however, osteogenesis may be protected in animals lacking PP5. This was further supported by the osteoblast development of BMSCs from mice in each group (Fig. 3H).

3.4. PP5 deficiency suppresses osteoclast differentiation and bone resorption in diabetic mice

The serum levels of RANKL (Fig. 4A–b, $P < 0.05$) and CTX-1C (Fig. 4A–a, $P < 0.01$) in KO-NC mice were considerably lower than in WT-NC mice, suggesting that PP5 KO mice had less bone resorption. When compared to WT-NC animals, the serum levels of CTX-1C (Fig. 4A–a, $P < 0.05$) and RANKL (Fig. 4A–b, $P < 0.001$) were considerably higher in WT-DM mice. Nevertheless, no statistically significant difference was observed in the serum levels of CTX-1C between KO-DM and KO-NC animals. Still, they were much lower than those of WT-DM mice (Fig. 4A–a, $P < 0.001$). While RANKL levels in the serum of KO-DM mice were higher than those of KO-NC animals (Fig. 4A–b, $P < 0.001$), they were still substantially lower than those of WT-DM mice (Fig. 4A–b, $P < 0.01$). In contrast to RANKL, OPG levels in the serum of KO-NC mice were significantly higher than those of WT-NC mice (Fig. 4A–c, $P < 0.001$). It did not alter compared to KO-DM and KO-NC mice, but it reduced significantly in WT-DM mice compared to WT-NC mice (Fig. 4A–c, $P < 0.05$). The factors mentioned above resulted in elevated RANKL/OPG ratios in WT-DM and WT-NC mice (Fig. 4A–d, $P < 0.001$), comparable RANKL/OPG ratios in KO-DM and WT-NC mice, higher RANKL/OPG ratios in WT-NC compared to KO-NC mice (Fig. 4A–d, $P < 0.01$), and elevated RANKL/OPG ratios in WT-DM, relative to KO-DM mice (Fig. 4A–d, $P < 0.001$). The *Rankl* and *Opg* levels variations correspond with protein levels (Fig. 4B–a, b). Additionally, the trend of *Nfatc1* levels downstream of RANKL/OPG is comparable to that of RANKL/OPG (Fig. 4B–c).

Tartrate-resistant acid phosphatase (TRAP) staining was used to examine changes in the osteoclast differentiation capacity of BMMs from mice in each group. Fig. 4C–a, c, E, F, $P < 0.05$ shows that the KO-NC group had considerably fewer and smaller osteoclasts (TRAP-positive) than the WT-NC group. As opposed to the WT-NC group, the number of osteoclasts in WT-DM group did not substantially alter (Fig. 4C–a, b, E); nevertheless, the average size of osteoclasts increased (Fig. 4C–a, b, F, $P < 0.001$). As seen in Fig. 4C–b, d, E, and F, the osteoclast number and area in the KO-DM group were comparable to those in the KO-NC group, but they were significantly fewer than those in the WT-DM group (number, $P < 0.01$; area, $P < 0.001$). To evaluate the ability of osteoclasts in each group to resorb bone, BMMs grown on slices of bovine bone were stimulated to develop into osteoclasts. Changes in the resorption pit area on the slices were then assessed. The resorption pit area in the WT-NC group was significantly higher than in the KO-NC group (Fig. 4D–a, c, G, $P < 0.05$), and it grew significantly in the WT-DM group (Fig. 4D–a, b, G, $P < 0.05$). The resorption pit area, however, did not change substantially between the KO-NC and KO-DM groups (Fig. 4D–c, d, G); however, it was significantly smaller in the KO-DM group than in the WT-DM group (Fig. 4D–b, d, G, $P < 0.001$). These findings are complemented by modifications in *in vitro* osteoclast development (Fig. 4C) and changes in bone resorption indicators (Fig. 4A).

3.5. PP5 deficiency indirectly suppresses osteoclast differentiation through osteoblasts

After PP5 loss, BMSCs and BMMs from WT and KO animals given a regular diet were co-cultured to examine the impact of osteoblasts on osteoclast development. The quantity ($P < 0.001$) and area ($P < 0.001$) of osteoclasts that developed in the KO BMSCs-KO BMMs co-culture system were significantly lower than in the WT BMSCs-WT BMMs co-culture system (Fig. 5A–a, d, e, and f). The number ($P < 0.001$) and area ($P < 0.001$) of osteoclasts rose significantly when WT BMSCs were co-cultured with KO BMMs in comparison to the KO BMSCs-KO BMMs co-culture system (Fig. 5A–b, d, e, and f). In contrast to the co-culture system of WT BMSCs-WT BMMs, the osteoclasts that differentiated in the KO BMSCs-WT BMMs were smaller ($P < 0.05$) and less numerous ($P < 0.001$) (Fig. 5A–a, c, e, f). These findings demonstrated that the osteoblasts that developed from the BMSCs of PP5 KO mice prevented the BMMs from differentiating into osteoclasts. Nevertheless, the osteoclasts that differentiated in the co-culture system of KO BMSCs-WT BMMs were presumably more ($P < 0.001$) and bigger ($P < 0.001$) than those that differentiated in the co-culture system of KO BMSCs-KO BMMs (Fig. 5A–c, d, e, and f), and the number ($P < 0.001$) and size ($P < 0.01$) of these osteoclasts were less than those of WT BMSCs-WT BMMs (Fig. 5A–a, b, e, and f). ELISA kits were used to detect changes in the levels of OPG and RANKL in the osteoblast culture media. Following PP5 knockout, RANKL concentrations were significantly ($P < 0.05$) lower (Fig. 5B–a), OPG levels were significantly ($P < 0.01$) higher (Fig. 5B–b), and the RANKL/OPG ratio was significantly ($P < 0.001$) lower (Fig. 5B–c). They all underwent in the opposite transformation when AA triggered PP5 (Fig. 5B).

4. Discussion

Increased cortical porosity, decreased cortical area, and decreased bone density are just a few of the detrimental effects of diabetes on the skeletal system that can impact an individual’s overall health by causing conditions like osteoporosis, bone fragility, and arthritis [1,2]. A high-fat diet cannot cause mice to gain weight, as previous research has demonstrated [18], and these mice have better blood glucose, regulation and glucose tolerance [19]. It is confirmed that PP5-deficient mice are resistant to high-fat diet-induced diabetes by the observation that, after a high-fat diet, the typical symptoms of diabetes, such as high blood glucose (Fig. 1C and D), impaired oral glucose tolerance (Fig. 1E), and insulin resistance (Fig. 1G), did not appear in PP5 KO mice. These findings are consistent with previous reports [18,19,21].

Normal indicators of osteoporosis were evident in WT mice with diabetic mellitus: a notable rise in Tb.Sp (Fig. 2H), Tb.Pf (Fig. 2I), SMI (Fig. 2J), and a noticeable decrease in BMD (Fig. 2E) and Tb.N (Fig. 2G). These alterations in WT mice’s bone structure align with findings by Lin et colleagues [30]. PP5 KO mice, on the other hand, did not show similar alteration when fed a high-fat diet, indicating that PP5 KO mice are resistant to osteoporosis in diabetic mice. Bone remodeling is essential for maintaining the integrity of bones in

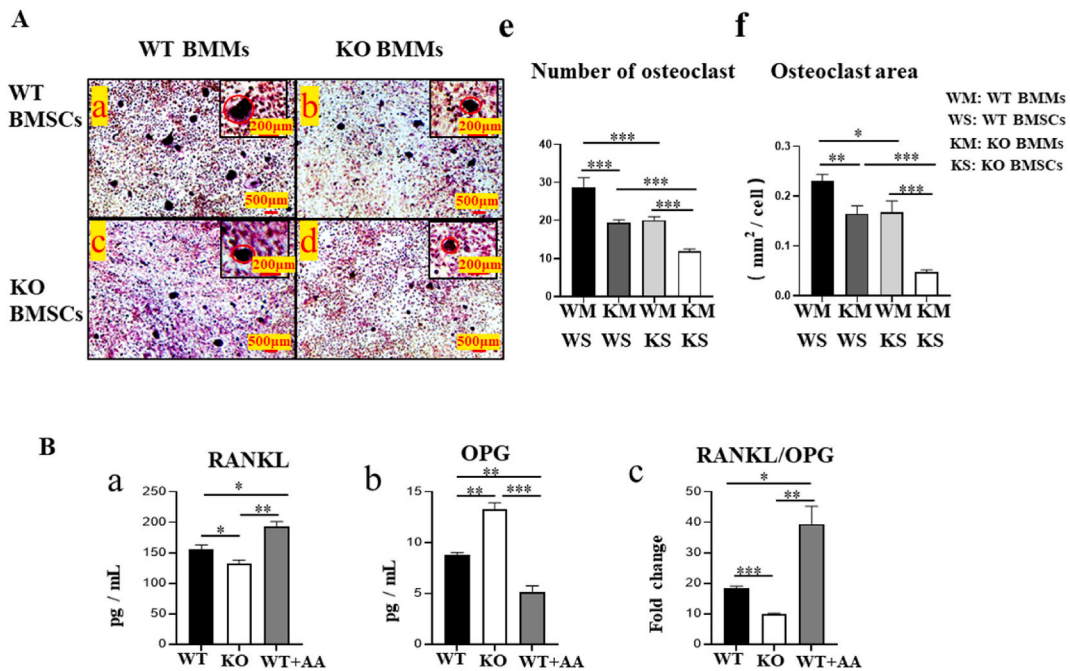


Fig. 5. Effect of mouse osteoblasts on osteoclast differentiation after PP5 deficiency. The BMSCs-BMMs co-culture system was used to detect the effect of osteoblasts on osteoclast differentiation after PP5 deficiency (A–a, b, c, and d). The differences in osteoclast number (within 80 mm²) and area (A–e and f) were statistically analyzed. The levels of RANKL (B–a), OPG (B–b) in culture medium of WT, KO osteoblasts and WT osteoblasts added with PP5 activator arachidonic acid (AA) were detected by ELISA kits, and the ratio of RANKL/OPG (B–c) was analyzed. Each value represents mean ± SD (n = 3). *: $P < 0.05$; **: $P < 0.01$; ***: $P < 0.001$; NS: $P > 0.05$.

mature mammals [31,32]. Osteoclasts mediate bone resorption in this process, while osteoblasts mediate bone formation [33–35]. Osteoporosis is a condition in which bone mass gradually diminishes due to excess bone resorption over bone production [36]. Our findings in WT mice with diabetic mellitus, showed that bone resorption significantly increased (Fig. 4A). In contrast, bone production dramatically decreased (Fig. 3A and B), which is consistent with the findings published by Zhu et al. [30,37,38]. These could cause osteoporosis in WT mice (Fig. 2). High-fat diet, however did not affect PP5 KO mice's bone resorption (Fig. 4A) or formation (Fig. 3A and B). PP5 KO mice avoid diabetes-induced osteoporosis, which may be primarily explained by this (Fig. 2).

In the process of forming bones, osteoblast differentiation is an essential phase. As demonstrated by PP5 deficiency in mice given a regular diet (Fig. 3H), this may improve bone formation (Fig. 3A and B) and is consistent with our prior findings [22]. Consistent with findings reported by Lin et al. [30], WT mice exhibit significantly reduced osteoblast differentiation after induced diabetes (Fig. 3H), which may result in decreased bone production (Fig. 3A and B). But as seen in Fig. 3H, animals lacking PP5 can withstand the loss in osteoblast differentiation brought on by a high-fat diet, which offsets the decline in bone production shown in Fig. 3A and B. During bone formation, RUNX2 plays a critical regulatory role in osteoblast differentiation [39–41]. Developmental abnormalities of the bones are caused by mutations in the *Runx2* gene [39,42]. According to reports, diabetes suppresses the expression of RUNX2 [30,43]. In the bone tissues of WT mice with diabetes mellitus, our study results demonstrate significant downregulation of RUNX2 expression (Fig. 3G). This could inhibit osteoblast differentiation by reducing the expression of downstream osteoblast markers, *Ocn* and *Bsp* (Fig. 3D and E), ultimately reducing bone formation [30,43]. Nonetheless, following a high-fat meal, PP5 KO mice's bone tissues show no appreciable change in RUNX2 expression (Fig. 3G). This could be because PP5 can dephosphorylate RUNX2 [22] and withstand hyperglycemia (Fig. 1-C, D). Therefore, PP5 KO mice might resist the decline in bone production observed in diabetic mice.

Since osteoclasts are the primary mediators of bone resorption, their ability to differentiate and resorb bone is essential. The ability of BMMs to develop into osteoclasts (Fig. 4C–E, F), and the ability of osteoclasts to resorb bone (Fig. 4D–G) is significantly inhibited by PP5 deficiency in our study, which may lead to decreased bone resorption in PP5 KO mice (Fig. 4A). And for this reason, the high-fat diet may not have been able to cause PP5 KO animals to exhibit increased bone resorption (Fig. 4A). The RANKL/OPG pathway controls osteoclast differentiation and maturation [44]. Tumor necrosis factor receptor-associated factors (TRAFs) are recruited to stimulate the transcription and expression of *Nfatc1*, an osteoclast marker, after RANKL's interaction with the receptor activator of NF- κ B (RANK) [45,46]. To suppress the RANKL-RANK signaling pathway and thus prevent osteoclast development and bone resorption, OPG can competitively bind to RANKL and prevent its combination with RANK [47]. Osteoclast differentiation and bone resorption capacity can be measured using the RANKL/OPG ratio, an essential variable [48]. PP5 deficiency reduces the RANKL/OPG signaling pathway, inhibiting osteoclast development and maturation. This may offset the increased bone resorption caused by a high-fat diet. RANKL and OPG are from osteoblast-related cells, which include MSCs, osteoblasts, and osteocytes [49]. Hence, increased osteogenesis could cause the PP5 KO mice's suppression of the RANKL/OPG signaling pathway. This theory is supported by the observation that osteoblasts derived from PP5 KO mice BMSCs prevented the BMMs from differentiating into osteoclasts (Fig. 5A) and that PP5 modulation of the RANKL/OPG ratio (Fig. 5B) underlies osteoblast culture medium. Osteoblasts derived from WT mouse BMSCs could not bring KO BMMs' osteoclast differentiation back to the same degree as WT BMMs (Fig. 5A–a, b, e, and f). It indicates that PP5 directly and indirectly affects osteoclast differentiation. Considering the contamination between BMMs and BMSCs, the co-culture of splenocytes and calvaria-derived osteoblasts warrants further investigation in the future.

In conclusion, we discovered that mice with high-fat diets do not develop osteoporosis because PP5 is absent. This is a first. Three mechanisms—preventing diabetes, promoting bone growth, and preventing bone resorption—may be used to accomplish this. However, additional investigation is necessary to examine the viability of using PP5 as a target for the management of diabetes and its associated osteoporosis.

Funding

This research was funded by the National Natural Science Foundation of China (82000791) and the Natural Science Foundation of Jiangsu Province (BK20220585).

Ethics statement

All animal experiments have been approved by the Ethics Committee of Yangzhou University. And the animal ethics permit number is NSFC2020-LPSPXY-3.

Data availability

Data will be made available on request.

CRedit authorship contribution statement

Jun Wang: Writing – original draft, Visualization, Validation, Supervision, Software, Resources, Methodology, Investigation, Funding acquisition, Formal analysis, Data curation, Conceptualization. **Changyu Zhao:** Writing – original draft, Software, Methodology, Investigation, Formal analysis, Data curation. **Wenpeng Zhao:** Investigation, Formal analysis, Data curation. **Songnan Li:** Writing – review & editing, Visualization, Supervision, Project administration, Funding acquisition, Conceptualization.

Declaration of competing interest

The authors declare that they have no known competing financial interests or personal relationships that could have appeared to influence the work reported in this paper.

Appendix A. Supplementary data

Supplementary data to this article can be found online at <https://doi.org/10.1016/j.heliyon.2024.e34027>.

References

- [1] J.N. Farr, M.T. Drake, S. Amin, L.J. Melton 3rd, L.K. McCready, S. Khosla, In vivo assessment of bone quality in postmenopausal women with type 2 diabetes, *J. Bone Miner. Res.* 29 (4) (2014) 787–795.
- [2] B. Lecka-Czernik, C.J. Rosen, Energy excess, glucose utilization, and skeletal remodeling: new insights, *J. Bone Miner. Res.* 30 (8) (2015) 1356–1361.
- [3] M. Saito, K. Marumo, Collagen cross-links as a determinant of bone quality: a possible explanation for bone fragility in aging, osteoporosis, and diabetes mellitus, *Osteoporos. Int.* 21 (2) (2010) 195–214.
- [4] T.J. Aspray, T.R. Hill, Osteoporosis and the ageing skeleton, *Subcell. Biochem.* 91 (2019) 453–476.
- [5] W. Liu, L.H. Yang, X.C. Kong, L.K. An, R. Wang, Meta-analysis of osteoporosis: fracture risks, medication and treatment, *Minerva Med.* 106 (4) (2015) 203–214.
- [6] J.A. Siddiqui, N.C. Partridge, Physiological bone remodeling: systemic regulation and growth factor involvement, *Physiology* 31 (3) (2016) 233–245.
- [7] L.J. Raggatt, N.C. Partridge, Cellular and molecular mechanisms of bone remodeling, *J. Biol. Chem.* 285 (33) (2010) 25103–25108.
- [8] P. Katsimbri, The biology of normal bone remodelling, *Eur. J. Cancer Care* 26 (6) (2017).
- [9] B. Lecka-Czernik, Diabetes, bone and glucose-lowering agents, basic biology, *Diabetologia* 60 (7) (2017) 1163–1169.
- [10] M.R. Rubin, Bone cells and bone turnover in diabetes mellitus, *Curr. Osteoporos. Rep.* 13 (3) (2015) 186–191.
- [11] F. Sassi, I. Buondonno, C. Luppi, E. Spertino, E. Stratta, M. Di Stefano, M. Ravazzoli, G. Isaia, M. Trento, P. Passera, M. Porta, G.C. Isaia, P. D'Amelio, Type 2 diabetes affects bone cells precursors and bone turnover, *BMC Endocr. Disord.* 18 (1) (2018) 55.
- [12] A. Donat, P.R. Knapstein, S. Jiang, A. Baranowsky, T.M. Ballhause, K.H. Frosch, J. Keller, Glucose metabolism in osteoblasts in healthy and pathophysiological conditions, *Int. J. Mol. Sci.* 22 (8) (2021).
- [13] M.R. Rubin, L.H. de Boer, J.C. Backlund, V. Arends, R. Gubitosi-Klug, A. Wallia, N. Sinha Gregory, A. Barnie, A.J. Burghardt, J.M. Lachin, B.H. Braffett, A. V. Schwartz, Biochemical markers of bone turnover in older adults with type 1 diabetes, *J. Clin. Endocrinol. Metab.* 107 (6) (2022) e2405–e2416.
- [14] M. Grotta, M.R. Rubin, J.P. Bilezikian, Anabolic skeletal therapy for osteoporosis, *Arq. Bras. Endocrinol. Metabol.* 50 (4) (2006) 745–754.
- [15] J. Green, G. Czanner, G. Reeves, J. Watson, L. Wise, V. Beral, Oral bisphosphonates and risk of cancer of oesophagus, stomach, and colorectum: case-control analysis within a UK primary care cohort, *Bmj* 341 (2010) e4444.
- [16] C. Ohlsson, D. Mellström, D. Carlzon, E. Orwoll, O. Ljunggren, M.K. Karlsson, L. Vandenput, Older men with low serum IGF-1 have an increased risk of incident fractures: the MrOS Sweden study, *J. Bone Miner. Res.* 26 (4) (2011) 865–872.
- [17] R.G. Bach, M.M. Brooks, M. Lombardero, S. Genuth, T.W. Donner, A. Garber, L. Kennedy, E.S. Monrad, R. Pop-Busui, S.F. Kelsey, R.L. Frye, Rosiglitazone and outcomes for patients with diabetes mellitus and coronary artery disease in the Bypass Angioplasty Revascularization Investigation 2 Diabetes (BARI 2D) trial, *Circulation* 128 (8) (2013) 785–794.
- [18] J. Wang, B. Qiu, M. Liu, C. Wang, W. Yong, Z. Xie, The effect of protein phosphatase 5 (PP5) on fat metabolism in mice, *Chin. J. Comp. Med.* (8) (2016) 79–84.
- [19] N. Grankvist, L. Amable, R.E. Honkanen, A. Sjöholm, H. Ortsäter, Serine/threonine protein phosphatase 5 regulates glucose homeostasis in vivo and apoptosis signalling in mouse pancreatic islets and clonal MIN6 cells, *Diabetologia* 55 (7) (2012) 2005–2015.
- [20] T.D. Hinds Jr., L.A. Stechschulte, H.A. Cash, D. Whisler, A. Banerjee, W. Yong, S.S. Khuder, M.K. Kaw, W. Shou, S.M. Najjar, E.R. Sanchez, Protein phosphatase 5 mediates lipid metabolism through reciprocal control of glucocorticoid receptor and peroxisome proliferator-activated receptor-γ (PPARγ), *J. Biol. Chem.* 286 (50) (2011) 42911–42922.
- [21] N. Grankvist, R.E. Honkanen, Å. Sjöholm, H. Ortsäter, Genetic disruption of protein phosphatase 5 in mice prevents high-fat diet feeding-induced weight gain, *FEBS Lett.* 587 (23) (2013) 3869–3874.
- [22] J. Wang, Y. Cao, B. Qiu, J. Du, T. Wang, C. Wang, R. Deng, X. Shi, K. Gao, Z. Xie, W. Yong, Ablation of protein phosphatase 5 (PP5) leads to enhanced both bone and cartilage development in mice, *Cell Death Dis.* 9 (2) (2018) 214.
- [23] W. Yong, S. Bao, H. Chen, D. Li, E.R. Sánchez, W. Shou, Mice lacking protein phosphatase 5 are defective in ataxia telangiectasia mutated (ATM)-mediated cell cycle arrest, *J. Biol. Chem.* 282 (20) (2007) 14690–14694.
- [24] X. Tong, J. Gu, R. Song, D. Wang, Z. Sun, C. Sui, C. Zhang, X. Liu, J. Bian, Z. Liu, Osteoprotegerin inhibit osteoclast differentiation and bone resorption by enhancing autophagy via AMPK/mTOR/p70S6K signaling pathway in vitro, *J. Cell. Biochem.* 120 (2) (2019) 1630–1642.
- [25] X. Tong, C. Zhang, D. Wang, R. Song, Y. Ma, Y. Cao, H. Zhao, J. Bian, J. Gu, Z. Liu, Suppression of AMP-activated protein kinase reverses osteoprotegerin-induced inhibition of osteoclast differentiation by reducing autophagy, *Cell Prolif.* 53 (1) (2020) e12714.
- [26] X. Jiang, M. Ye, X. Jiang, G. Liu, S. Feng, L. Cui, H. Zou, Method development of efficient protein extraction in bone tissue for proteome analysis, *J. Proteome Res.* 6 (6) (2007) 2287–2294.
- [27] Y.L. Ma, M. Hamang, J. Lucchesi, N. Bivi, Q. Zeng, M.D. Adrian, S.E. Raines, J. Li, S.A. Kuhstoss, V. Obungu, H.U. Bryant, V. Krishnan, Time course of disassociation of bone formation signals with bone mass and bone strength in sclerostin antibody treated ovariectomized rats, *Bone* 97 (2017) 20–28.
- [28] H. Zwickl, E. Zwickl-Traxler, A. Haushofer, J. Seier, K. Podar, M. Weber, K. Hackner, N. Jacobi, M. Pecherstorfer, S. Vallet, Effect of cachexia on bone turnover in cancer patients: a case-control study, *BMC Cancer* 21 (1) (2021) 744.
- [29] Y. Yang, G. Liu, Y. Zhang, G. Xu, X. Yi, J. Liang, C. Zhao, J. Liang, C. Ma, Y. Ye, M. Yu, X. Qu, Association between bone mineral density, bone turnover markers, and serum cholesterol levels in type 2 diabetes, *Front. Endocrinol.* 9 (2018) 646.
- [30] Y. Lin, X. Shen, Y. Ke, C. Lan, X. Chen, B. Liang, Y. Zhang, S. Yan, Activation of osteoblast ferroptosis via the METTL3/ASK1-p38 signaling pathway in high glucose and high fat (HGHF)-induced diabetic bone loss, *Faseb j* 36 (3) (2022) e22147.
- [31] J.S. Kenkre, J. Bassett, The bone remodelling cycle, *Ann. Clin. Biochem.* 55 (3) (2018) 308–327.
- [32] K. Henriksen, M.A. Karsdal, T.J. Martin, Osteoclast-derived coupling factors in bone remodeling, *Calcif. Tissue Int.* 94 (1) (2014) 88–97.
- [33] J. Delgado-Calle, T. Bellido, The osteocyte as a signaling cell, *Physiol. Rev.* 102 (1) (2022) 379–410.
- [34] X. Chen, W. Wang, N. Duan, G. Zhu, E.M. Schwarz, C. Xie, Osteoblast-osteoclast interactions, *Connect. Tissue Res.* 59 (2) (2018) 99–107.
- [35] Z. Li, K. Kong, W. Qi, Osteoclast and its roles in calcium metabolism and bone development and remodeling, *Biochem. Biophys. Res. Commun.* 343 (2) (2006) 345–350.
- [36] J.Y. Noh, Y. Yang, H. Jung, Molecular mechanisms and emerging therapeutics for osteoporosis, *Int. J. Mol. Sci.* 21 (20) (2020).
- [37] A.L. Carvalho, V.E. DeMambro, A.R. Guntur, P. Le, K. Nagano, R. Baron, F.J.A. de Paula, K.J. Motyl, High fat diet attenuates hyperglycemia, body composition changes, and bone loss in male streptozotocin-induced type 1 diabetic mice, *J. Cell. Physiol.* 233 (2) (2018) 1585–1600.

- [38] R. Zhu, Z. Wang, Y. Xu, H. Wan, X. Zhang, M. Song, H. Yang, Y. Chai, B. Yu, High-fat diet increases bone loss by inducing ferroptosis in osteoblasts, *Stem Cells Int* 2022 (2022) 9359429.
- [39] T. Komori, H. Yagi, S. Nomura, A. Yamaguchi, K. Sasaki, K. Deguchi, Y. Shimizu, R.T. Bronson, Y.H. Gao, M. Inada, M. Sato, R. Okamoto, Y. Kitamura, S. Yoshiki, T. Kishimoto, Targeted disruption of *Cbfa1* results in a complete lack of bone formation owing to maturational arrest of osteoblasts, *Cell* 89 (5) (1997) 755–764.
- [40] H. Qin, J. Cai, Effect of *Runx2* silencing on autophagy and RANKL expression in osteoblasts, *Arch. Oral Biol.* 95 (2018) 74–78.
- [41] Y. Ikebuchi, S. Aoki, M. Honma, M. Hayashi, Y. Sugamori, M. Khan, Y. Kariya, G. Kato, Y. Tabata, J.M. Penninger, N. Udagawa, K. Aoki, H. Suzuki, Coupling of bone resorption and formation by RANKL reverse signalling, *Nature* 561 (7722) (2018) 195–200.
- [42] K.W. McLarren, R. Lo, D. Grbavec, K. Thirunavukkarasu, G. Karsenty, S. Stifani, The mammalian basic helix loop helix protein HES-1 binds to and modulates the transactivating function of the runt-related factor *Cbfa1*, *J. Biol. Chem.* 275 (1) (2000) 530–538.
- [43] J.L. Fowlkes, R.C. Bunn, L. Liu, E.C. Wahl, H.N. Coleman, G.E. Cockrell, D.S. Perrien, C.K. Lumpkin Jr., K.M. Thrailkill, Runt-related transcription factor 2 (*RUNX2*) and *RUNX2*-related osteogenic genes are down-regulated throughout osteogenesis in type 1 diabetes mellitus, *Endocrinology* 149 (4) (2008) 1697–1704.
- [44] F. Xu, Y. Dong, X. Huang, P. Chen, F. Guo, A. Chen, S. Huang, Pioglitazone affects the OPG/RANKL/RANK system and increase osteoclastogenesis, *Mol. Med. Rep.* 14 (3) (2016) 2289–2296.
- [45] H. Takayanagi, RANKL as the master regulator of osteoclast differentiation, *J. Bone Miner. Metabol.* 39 (1) (2021) 13–18.
- [46] A. Anesi, L. Generali, L. Sandoni, S. Pozzi, A. Grande, From osteoclast differentiation to osteonecrosis of the jaw: molecular and clinical insights, *Int. J. Mol. Sci.* 20 (19) (2019) 4925.
- [47] Y. Zhang, J. Liang, P. Liu, Q. Wang, L. Liu, H. Zhao, The RANK/RANKL/OPG system and tumor bone metastasis: potential mechanisms and therapeutic strategies, *Front. Endocrinol.* 13 (2022) 1063815.
- [48] J. Zhao, M. Huang, X. Zhang, J. Xu, G. Hu, X. Zhao, P. Cui, X. Zhang, MiR-146a deletion protects from bone loss in OVX mice by suppressing RANKL/OPG and M-CSF in bone microenvironment, *J. Bone Miner. Res.* 34 (11) (2019) 2149–2161.
- [49] T. Nakashima, M. Hayashi, T. Fukunaga, K. Kurata, M. Oh-hora, J.Q. Feng, L.F. Bonewald, T. Kodama, A. Wutz, E.F. Wagner, J.M. Penninger, H. Takayanagi, Evidence for osteocyte regulation of bone homeostasis through RANKL expression, *Nat. Med.* 17 (10) (2011) 1231–1234.